Weather and climate analyses using improved global water vapor observations

Thomas H. Vonder Haar,[1,2] Janice L. Bytheway,[1,2] and John M. Forsythe[1,3]

[1]   The NASA Water Vapor Project (NVAP) dataset is a global (land and ocean) water vapor dataset created by merging multiple sources of atmospheric water vapor to form a global data base of total and layered precipitable water vapor. Under the NASA Making Earth Science Data Records for Research Environments (MEaSUREs) program, NVAP is being reprocessed and extended, increasing its 14-year coverage to include 22 years of data. The NVAP-MEaSUREs (NVAP-M) dataset is geared towards varied user needs, and biases in the original dataset caused by algorithm and input changes were removed. This is accomplished by relying on peer reviewed algorithms and producing the data in multiple "streams" to create products geared towards studies of both climate and weather. We briefly discuss the need for reprocessing and extension, steps taken to improve the product, and provide some early science results highlighting the improvements and potential scientific uses of NVAP-M. **Citation:** Vonder Haar, T. H., J. L. Bytheway, and J. M. Forsythe (2012), Weather and climate analyses using improved global water vapor observations, *Geophys. Res. Lett.*, *39*, L15802, doi:10.1029/2012GL052094.

1. Introduction

[2]   Water vapor is a principal atmospheric variable, and is a central component in both the Earth Energy Budget and the Global Water Cycle. Clouds and precipitation manifest its presence, its phase transitions are a source of energy to influence motions in the atmosphere, and its transport (e.g., atmospheric rivers [*Newell et al.*, 1992; *Ralph et al.*, 2006]) can produce significant weather events. Increasing water vapor amounts in a warming climate could accelerate the global hydrologic cycle [*Wentz et al.*, 2007].

[3]   Understanding the nonlinear dynamics of Earth's climate system requires new knowledge of water vapor variability and its long-acknowledged feedback mechanisms [*Intergovernmental Panel on Climate Change*, 2007; *Sherwood et al.*, 2009; *Soden et al.*, 2005; *Pierrehumbert*, 2010]. Despite its importance, quantifying the distribution of global water vapor is challenged by the limits of individual observational tools. Radiosonde and surface-based Global Positioning System (GPS) networks are weighted towards continents and the Northern Hemisphere, while the passive microwave record of total precipitable water (TPW) from satellites is generally limited to oceans only [*Mears et al.*, 2007]. Hyperspectral infrared water vapor retrievals from satellites are limited and affected by clouds [*Fetzer et al.*, 2006].

[4]   This paper presents the first analyses from a new, 22-year observational global water vapor dataset. Results provide some of the new information required for climate and weather science, as well as introduce the new dataset to the user community.

[5]   The need for a blended multisensor water vapor product led to the creation of the NASA Water Vapor Project (NVAP) dataset [*Randel et al.*, 1996; *Vonder Haar et al.*, 2003]. NVAP is a 14-year (1988–2001) dataset of daily, 1-degree gridded TPW and layered precipitable water (LPW) over both ocean and land that has been used to study a variety of weather and climate phenomena, including the Madden-Julian Oscillation (MJO) [*Maloney and Esbensen*, 2003], monsoons [*Fasullo and Webster*, 2003], and model performance [*Norris and Weaver*, 2001].

[6]   NVAP was produced in three separate phases between 1992 and 2003, resulting in the existing dataset (hereafter "heritage NVAP"). NVAP (1988–1999) included infrared (Television Infrared Operational Satellite (TIROS) Operational Vertical Sounder (TOVS)) and microwave (Special Sensor Microwave /Imager (SSM/I)) satellite data blended with soundings from radiosondes. The "next generation" dataset (NVAP-NG, 2000–2001) added data from the Advanced Microwave Sounding Unit (AMSU) and Special Sensor Microwave/Temperature-2 (SSM/T2). Areas with no or missing data were filled using spatial and temporal interpolation techniques, and a data source code accompanying the dataset indicated whether a value was observed or interpolated.

[7]   Changes to input datasets and selected algorithms were made with each phase of processing, incorporating improved data and processing methodologies, but resulting in several time-dependent artifacts that degraded the dataset's decadal uniformity. These changes, in combination with the dataset's relatively short period of record, make the heritage NVAP dataset unsuitable for long-term trend analysis [*Trenberth et al.*, 2005].

[8]   As part of the NASA Making Earth Science Data Records for Use in Research Environments (MEaSUREs) program, heritage NVAP is being reprocessed for the first time, and temporally extended to cover 1988–2009. The resulting dataset, NVAP-MEaSUREs (NVAP-M), expands the temporal coverage of heritage NVAP and improves the analysis, creating a record of Earth's water vapor on various timescales.

[1]METSAT Division, Science and Technology Corporation, Laporte, Colorado, USA.
[2]Department of Atmospheric Science, Colorado State University, Fort Collins, Colorado, USA.
[3]Cooperative Institute for Research in the Atmosphere, Colorado State University, Fort Collins, Colorado, USA.

Corresponding author: T. H. Vonder Haar, METSAT Division, Science and Technology Corporation, 4033 Buckskin Trl., Laporte, CO 80535, USA. (vonderhaar@cira.colostate.edu)

Table 1. Assigned Variances Used for Weighted Merging

	SSM/I	HIRS	Radiosonde	GPS	AIRS
Variance (mm)	3.0	10.0	2.0	1.0	3.0

[9] In contrast to the single product of the heritage NVAP dataset, NVAP-M was produced in three independent "tiers": NVAP-M Climate, NVAP-M Weather, and NVAP-M Ocean, each tailored for specific user needs. NVAP-M Climate provides daily, land and ocean, 1° gridded TPW and LPW, representing the most stable water vapor dataset over time for use in climate applications. NVAP-M Weather provides 6-hourly, 0.5° gridded TPW and LPW for use in studies of shorter time scales and weather case studies. NVAP-M Ocean is similar to NVAP-M Climate, using only TPW data from SSM/I, and is intended to mirror other microwave ocean-only water vapor datasets [e.g., *Mears et al.*, 2007].

[10] This paper focuses mainly on NVAP-M Climate, briefly outlining its production and results. The differences between the weather and climate product will be discussed.

2. Methods

2.1. Data Sources and Retrieval Algorithms

[11] Heritage NVAP was created with no model input, and NVAP-M continues this practice with the exception of the NASA Modern Era Retrospective Analysis for Research Applications (MERRA) [*Rienecker et al.*, 2011], which provides a priori temperature profiles in the infrared retrieval algorithm but has no direct influence on the final product. NVAP-M uses published radiance inputs that have been intercalibrated and quality controlled to ensure consistency between data from like instruments flying on multiple satellite platforms (for a general discussion of satellite characteristics, see *Kidder and Vonder Haar* [1995]). The input sources for all NVAP-M products are the same, with the exception of TPW retrievals from GPS radio occultation measurements [*Wang et al.*, 2007] added to the NVAP-M Weather product beginning in 1995. A timeline of instruments used in NVAP-M Climate is shown in the auxiliary material.[1]

[12] SSM/I is the core instrument for oceanic observations in all versions of heritage NVAP and NVAP-M. Intercalibrated SSM/I brightness temperatures [*Sapiano et al.*, 2012] are used in the parametric retrieval algorithm described by *Elsaesser and Kummerow* [2008] and based on the optimal estimation (OE) technique outlined by *Rodgers* [2000] to retrieve TPW over oceanic scenes.

[13] The HIRS instrument, available on the polar-orbiting NOAA satellites, is also used in all versions of NVAP-M. HIRS can retrieve water vapor information over land, and supplies vertical structure information. The OE retrieval of *Engelen and Stephens* [1999] is applied to quality-controlled, clear-sky HIRS spectral radiance channels 8, 10, 11, and 12 [*Jackson and Bates*, 2000; *Jackson et al.*, 2003], resulting in LPW in four layers (surface to 700-hPa, 700–500 hPa, 500–300 hPa, and <300 hPa) that match the layers used in heritage NVAP. Temperature profiles at 100 hPa vertical spacing are supplied every three hours from the NASA MERRA dataset [*Rienecker et al.*, 2011], representing NVAP-M's only direct dependence on numerical model information.

---

[1]Auxiliary materials are available in the HTML. doi:10.1029/2012GL052094.

[14] Water vapor retrievals from the Atmospheric Infrared Sounder (AIRS) became available in 2002, and Version 5, Level 2 and 3 total column and layered water vapor data [*Aumann et al.*, 2003; *Fetzer et al.* 2006] are merged directly into both NVAP-M Weather and Climate products. A 1° resolution LPW (4 layers) and covariance climatology derived from AIRS clear sky retrievals for 2003–2009 is also used as *a priori* information in the HIRS retrieval algorithm, allowing the AIRS climatology to back-propagate into the pre-AIRS era.

[15] Quality-controlled radiosonde soundings from the Integrated Global Radiosonde Archive (IGRA) [*Durre and Yin*, 2008] are also used in NVAP-M Climate and Weather.

2.2. Merging Process

[16] The data merging process is the same for all production streams, altering only the spatial and temporal resolution. The SSM/I and HIRS retrievals are performed on each field of view, and then averaged onto a 1.0° (NVAP-M Climate, NVAP-M Ocean) or 0.5° (NVAP-M Weather) grid. This results in gridded TPW and LPW maps for each available SSM/I, HIRS, and AIRS. A single radiosonde or GPS data point is assumed to represent the grid box it occupies; or, if multiple data points are available within a grid box, they are averaged. Gridded TPW and LPW from like sensors are averaged together, resulting in a single TPW and LPW map for each platform.

[17] An error-weighted averaging technique combines all available TPW/LPW observations for a given day (or 6-hour period for NVAP-M Weather). Each sensor platform is assigned a variance based on comparisons with other observations or from published values (Table 1) which determines the sensor's assigned weight:

$$w_i = \frac{1}{\sigma_i^2} \qquad (1)$$

where w_i is the weight assigned to the observation from instrument i and σ^2 is the variance of the sensor. TPW for the grid box is then calculated as:

$$\overline{TPW} = \frac{\sum_{i=1}^{N} w_i v_i}{\sum_{i=1}^{N} w_i} \qquad (2)$$

where v_i represents the average water vapor in a given grid box from instrument i.

[18] A similar weighting process creates the 4-layer LPW field. Due to the combination of observations from multiple sensors, it is possible that the sum of the LPW in a grid box value will not equal the TPW value calculated for the same grid box and time. TPW, due to its use of the GPS and SSM/I, is considered more reliable than LPW.

3. Results

3.1. Improvement Over Heritage NVAP

[19] NVAP-M contains many major improvements over the heritage NVAP dataset, such that these results completely supersede those presented by *Randel et al.* [1996] and the statistics compiled by *Amenu and Kumar* [2005]. Figure 1 demonstrates the improved decadal stability of
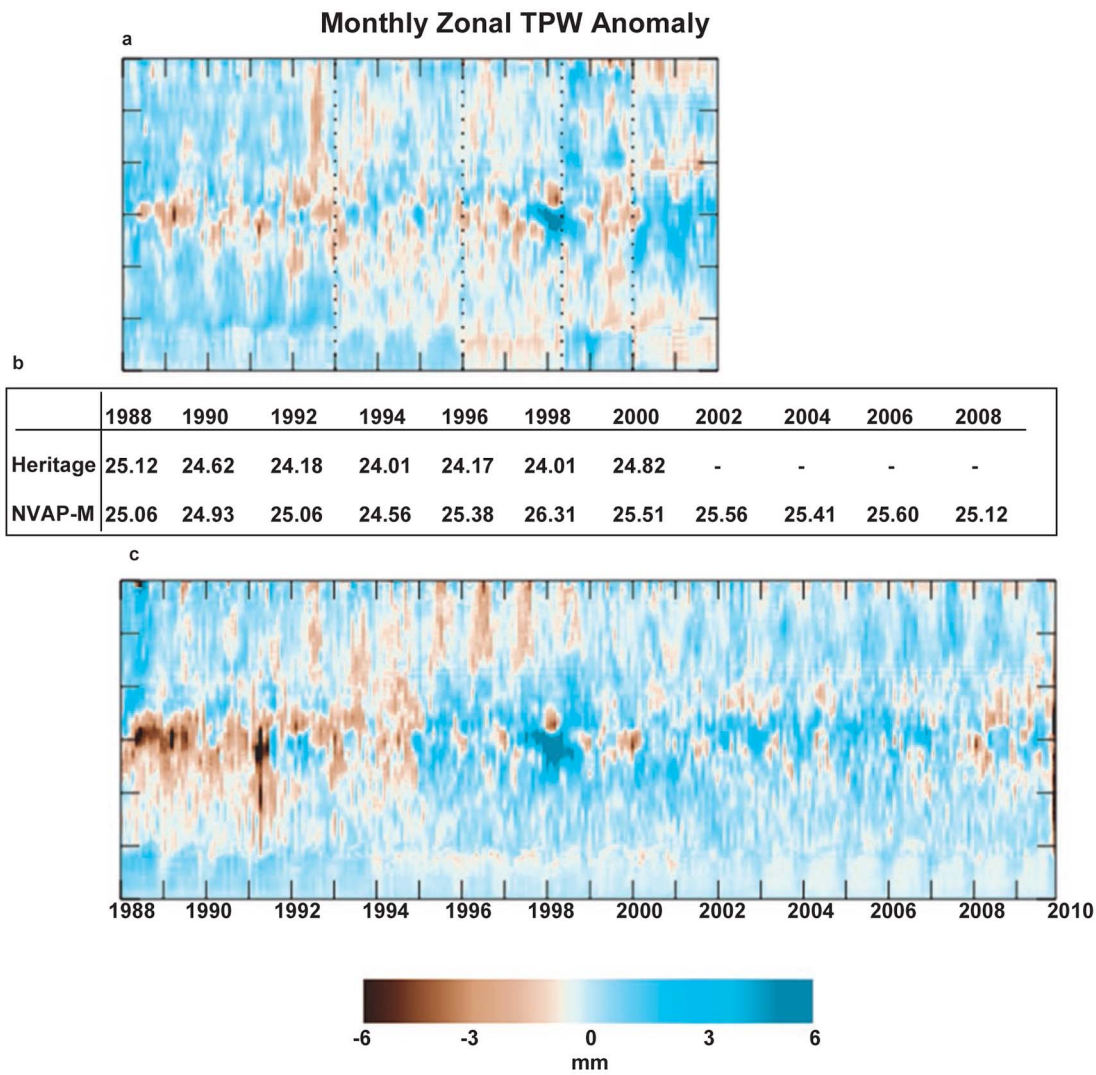
Monthly Zonal TPW Anomaly

	1988	1990	1992	1994	1996	1998	2000	2002	2004	2006	2008
Heritage	25.12	24.62	24.18	24.01	24.17	24.01	24.82	-	-	-	-
NVAP-M	25.06	24.93	25.06	24.56	25.38	26.31	25.51	25.56	25.41	25.60	25.12

Figure 1. Monthly zonal water vapor anomalies from (a) heritage NVAP, with time-dependent biases indicated by dotted lines, and (c) NVAP-M. The known biases have been removed from the NVAP-M dataset. (b) The global monthly average TPW for even numbered years for each dataset.

NVAP-M over the heritage dataset, comparing the zonal water vapor anomalies of each dataset, referenced to itself.

[20] Time dependent biases in the heritage dataset are indicated by a dotted line in Figure 1a. The use of peer-reviewed algorithms and intercalibrated data sources with long periods of availability to reprocess the heritage dataset removes these biases in the improved NVAP-M dataset (Figure 1c.) and provides a more stable record of global water vapor. Not all artifacts are completely removed, however. The tropical dry bias in the early part of the record, as well as the global moistening in 1995, are the result of changes in satellite sampling with time (see auxiliary material for discussion).

[21] Figure 1b displays a table of the global average water vapor for every other year (full table in auxiliary material) for both the heritage and NVAP-M datasets. Despite the appearance of biases in Figures 1a and 1c, Figure 1b indicates that the global mean TPW variability is less than 10% of the overall dataset mean value (24.56 mm for heritage NVAP; 25.37 mm for NVAP-M).
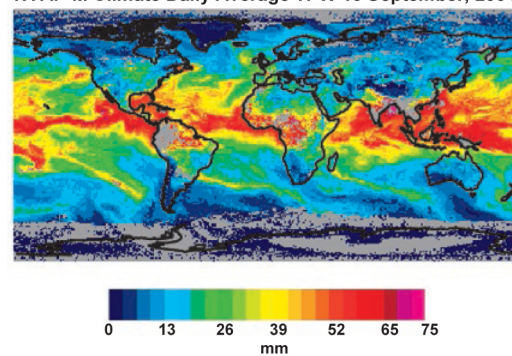

Figure 2. Global daily average TPW from NVAP-M Climate for 10 September, 2004. No interpolation was performed to fill areas of persistently cloudy or missing data, depicted by grey regions.
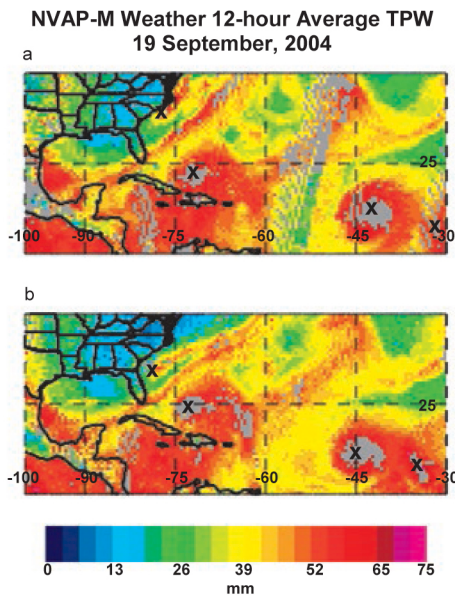
NVAP-M Weather 12-hour Average TPW
19 September, 2004

Figure 3. 12-hourly composite of NVAP-M Weather showing the average TPW for (a) 0000–1159 UTC and (b) 1200–2359 UTC on 19 September, 2004 over the western North Atlantic Ocean and eastern United States. Note the water vapor associated with several tropical cyclones, denoted by Xs. Clockwise from the southeastern corner are: Tropical Storm Lisa, Hurricane Karl, Hurricane Jeanne, and Hurricane Ivan.

3.2. Early Science Results: Weather and Climate Studies

[22] NVAP-M provides a record of TPW and LPW suitable for studying a variety of atmospheric phenomena, on a variety of timescales. Figures 2 and 3 show results of NVAP-M Climate and NVAP-M Weather. Figure 2 displays the NVAP-M Climate daily average TPW for 10 September 2004. The highest values of TPW are found over the tropics and oceans, decreasing towards the poles and over the continents, particularly in high elevations. Transport of atmospheric water vapor by atmospheric rivers is seen in both the northern Pacific and Atlantic Oceans. Examples of NVAP-M Climate LPW and NVAP-M Ocean for the same day shown in Figure 2 are shown in the auxiliary material.

[23] Figure 3 is an example of NVAP-M Weather over the Atlantic Ocean and eastern North America. The higher spatial and temporal resolution of NVAP-M Weather allows for studies of water vapor variability and extreme weather phenomena as they evolve.

3.3. Early Science Results: Global Variability

[24] NVAP-M Climate is designed for studies on seasonal to interannual timescales on various spatial scales. The first new results on the 22-year annual cycle are shown in Figure 4. Panels a and b show monthly average TPW for January and July of 2009, respectively. Seasonal variation is evident in the migration of the thermal equator, and the distribution of water vapor over the northern hemisphere exhibits the largest seasonal variability, particularly in Canada and Russia. The Indian sub-continent also exhibits large seasonal variability, with large amounts of moisture present during the summer monsoon season that are not seen in the winter months.

[25] Figure 4c demonstrates the annual variability of TPW from 1988–2009 and shows yearly seasonal variations as well as circulations occurring on larger time scales. For example, the strong El Nino of 1997–1998 is signified by higher monthly global average TPW for the duration of the event. Again, artifacts due to time-space satellite sampling are discussed in the auxiliary material.
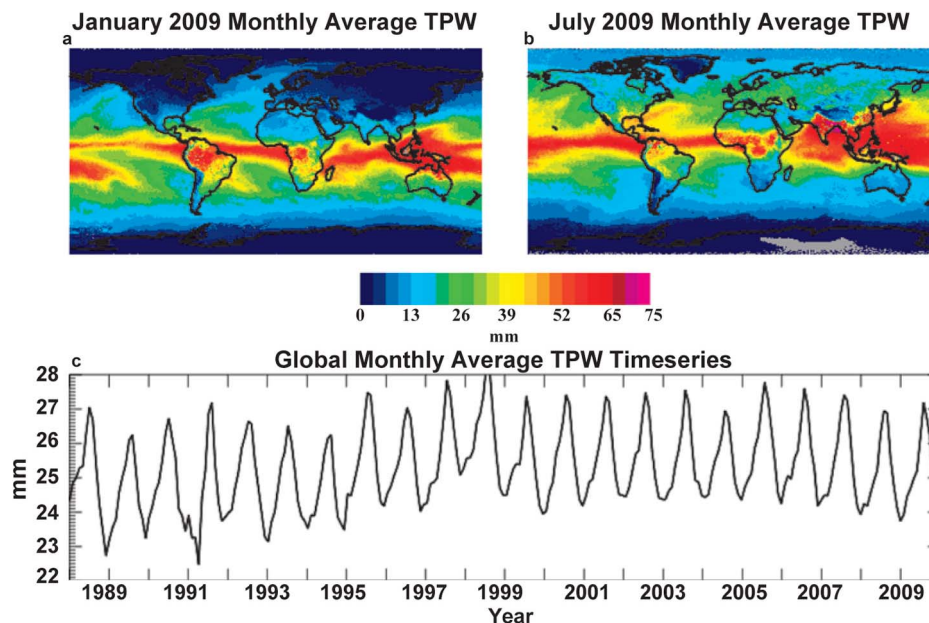

Figure 4. Seasonal and interannual variability from NVAP-M Climate: monthly average TPW for (a) January and (b) July 2009. (c) The global monthly average TPW.
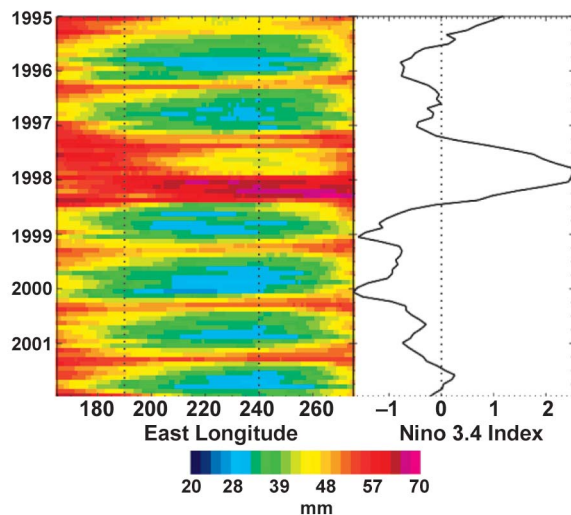
Figure 5. (left) Average TPW in the zonal band from 5°N to 5°S over the Pacific ocean illustrates not only the seasonal cycle of water vapor in the region as caused by the migration of the ITCZ, but also (right) the effect of the El Nino Southern Oscillation (ENSO) cycle on the distribution of water vapor in this region. Dotted lines represent the longitudinal boundaries of the Nino 3.4 region.

[26] The impacts of El Nino and La Nina on the distribution of tropical water vapor can also be seen in Figure 5, showing the average water vapor in the Pacific Ocean from 5°N–5°S and the monthly Nino 3.4 index [*Trenberth*, 1997] for 7 years from 1995–2001. In 1995–1996, ENSO is in a neutral or weak La Nina phase, with relatively dry conditions in the central Pacific and increased moisture in the west Pacific warm pool. In 1997, the Nino 3.4 index increases towards a strong positive phase and water vapor over the warm pool also increases. Increased water vapor then migrates eastward for the duration of the ENSO event. In 1999, ENSO moves to a moderate La Nina phase, with somewhat drier conditions in the warm pool than those observed during the more neutral phase in 1995–1996. In late 2000, ENSO neutral conditions resume.

4. Conclusions

[27] The heritage NVAP global water vapor dataset has long served as a useful mechanism for studies of water vapor interactions with various atmospheric phenomena. Inconsistent processing phases and their associated impact on the dataset, however, made the heritage dataset less-than-ideal for studies of interannual variability and climate. Reprocessing the dataset for NVAP-M has improved the quality and temporal consistency of the dataset and extended the record into the current era of hyperspectral soundings. The use of multiple production streams makes the dataset suitable for a variety of studies on a variety of spatial and temporal scales.

[28] The results of Figures 1 and 4 have not been subjected to detailed global or regional trend analyses, which will be a topic for a forthcoming paper. Such analyses must account for the changes in satellite sampling discussed in the auxiliary material. Therefore, at this time, we can neither prove nor disprove a robust trend in the global water vapor data. NVAP-M and its associated detailed documentation

and metadata will be available in mid-2012 at the NASA Langley Atmospheric Science Data Center (ASDC).

References

Amenu, G. G., and P. Kumar (2005), NVAP and Reanalysis-2 global precipitable water products: Intercomparison and variability studies, *Bull. Am. Meteorol. Soc.*, *86*, 245–256, doi:10.1175/BAMS-86-2-245.

Aumann, H. H., et al. (2003), AIRS/AMSU/HSB on the Aqua mission: Design, science objectives, data products, and processing systems, *IEEE Trans. Geosci. Remote Sens.*, *41*(2), 253–264, doi:10.1109/TGRS.2002.808356.

Durre, I., and X. Yin (2008), Enhanced radiosonde data for studies of vertical structure, *Bull. Am. Meteorol. Soc.*, *89*, 1257–1262, doi:10.1175/2008BAMS2603.1.

Elsaesser, G. S., and C. D. Kummerow (2008), Towards a fully parametric retrieval of the non-raining parameters over the global ocean, *J. Appl. Meteorol. Climatol.*, *47*, 1599–1618, doi:10.1175/2007JAMC1712.1.

Engelen, R. J., and G. L. Stephens (1999), Characterization of water-vapour retrievals from TOVS/HIRS and SSM/T2 measurements, *Q. J. R. Meteorol. Soc.*, *125*, 331–351, doi:10.1002/qj.49712555317.

Fasullo, J., and P. J. Webster (2003), A hydrological definition of Indian monsoon onset and withdrawal, *J. Clim.*, *16*, 3200–3211, doi:10.1175/1520-0442(2003)016<3200a:AHDOIM>2.0.CO;2.

Fetzer, E. J., B. H. Lambrigtsen, A. Eldering, H. H. Aumann, and M. T. Chahine (2006), Biases in total precipitable water vapor climatologies from Atmospheric Infrared Sounder and Advanced Microwave Scanning Radiometer, *J. Geophys. Res.*, *111*, D09S16, doi:10.1029/2005JD006598.

Intergovernmental Panel on Climate Change (2007), *Climate Change 2007: The Physical Science Basis. Contribution of Working Group I to the Fourth Assessment Report of the Intergovernmental Panel on Climate Change*, edited by S. Solomon et al., Cambridge Univ. Press, Cambridge, U. K.

Jackson, D. L., and J. J. Bates (2000), A 20-yr TOVS Pathfinder data set for climate analysis, paper presented at 10th Conference on Satellite Meteorology and Oceanography, Am. Meteorol. Soc., Long Beach, Calif.

Jackson, D. L., J. J. Bates, and D. Wylie (2003), The HIRS Pathfinder radiance data set (1979–2001). paper presented at 12th Conference on Satellite Meteorology and Oceanography, Am. Meteorol. Soc., Long Beach, Calif.

Kidder, S. Q., and T. H. Vonder Haar (1995), *Satellite Meteorology: An Introduction*, Academic, San Diego, Calif.

Maloney, E. D., and S. K. Esbensen (2003), The amplification of east Pacific Madden-Julian Oscillation convection and wind anomalies during June-November, *J. Clim.*, *16*, 3482–3497, doi:10.1175/1520-0442(2003)016<3482:TAOEPM>2.0.CO;2.

Mears, C. A., B. D. Santer, F. J. Wentz, K. E. Taylor, and M. F. Wehner (2007), Relationship between temperature and precipitable water changes over tropical oceans, *Geophys. Res. Lett.*, *34*, L24709, doi:10.1029/2007GL031936.

Newell, R. E., N. E. Newell, Y. Zhu, and C. Scott (1992), Tropospheric rivers?—A pilot study, *Geophys. Res. Lett.*, *19*(24), 2401–2404, doi:10.1029/92GL02916.

Norris, J. R., and C. P. Weaver (2001), Improved techniques for evaluating GCM cloudiness applied to the NCAR CCM3, *J. Clim.*, *14*, 2540–2550, doi:10.1175/1520-0442(2001)014<2540:ITFEGC>2.0.CO;2.

Pierrehumbert, R. T. (2010), *Principles of Planetary Climate*, Cambridge Univ. Press, Cambridge, U. K., doi:10.1017/CBO9780511780783.

Ralph, F. M., P. J. Neiman, G. A. Wick, S. I. Gutman, M. D. Dettinger, D. R. Cayan, and A. B. White (2006), Flooding on California's Russian River: Role of atmospheric rivers, *Geophys. Res. Lett.*, *33*, L13801, doi:10.1029/2006GL026689.

Randel, D. L., T. H. Vonder Haar, M. A. Ringerud, G. L. Stephens, T. J. Greenwald, and C. L. Combs (1996), A new global water vapor dataset, *Bull. Am. Meteorol. Soc.*, *77*, 1233–1246, doi:10.1175/1520-0477(1996)077<1233:ANGWVD>2.0.CO;2.

Rienecker, M. M., et al. (2011), MERRA-NASA's Modern-Era Retrospective Analysis for Research and Applications, *J. Clim.*, *24*, 3624–3648, doi:10.1175/JCLI-D-11-00015.1.

Rodgers, C. D. (2000), *Inverse Methods for Atmospheric Sounding: Theory and Practice*, World Sci., Singapore, doi:10.1142/9789812813718.

Sapiano, M. R. P., W. K. Berg, D. S. McKague, and C. D. Kummerow (2012), Towards an intercalibrated fundamental climate data record of the SSM/I sensors, *IEEE Trans. Geosci. Remote Sens.*, in press.

Sherwood, S. C., N. Andronova, E. Feter, and E. R. Kursinski (2009), What can water vapor reveal about past and future climate change?, *Eos Trans. AGU*, *90*(14), 122, doi:10.1029/2009EO140011.

Soden, B., D. L. Jackson, V. Ramaswamy, D. Schwarzkopf, and X. Huang (2005), The radiative signal of upper tropospheric moistening, *Science*, *310*, 841–844, doi:10.1126/science.1115602.

Trenberth, K. E. (1997), The definition of El Niño, *Bull. Am. Meteorol. Soc.*, *78*, 2771–2777, doi:10.1175/1520-0477(1997)078<2771:TDOENO>2.0. CO;2.

Trenberth, K. E., J. Fasullo, and L. Smith (2005), Trends and variability in column-integrated atmospheric water-vapor, *Clim. Dyn.*, *24*, 741–758, doi:10.1007/s00382-005-0017-4.

Vonder Haar, T. H., J. M. Forsythe, D. McKague, D. L. Randel, B. C. Ruston, and S. Woo (2003), Continuation of the NVAP Global Water Vapor Data Sets for Pathfinder science analysis, *STC Tech. Rep. 3333*, Sci. and Technol. Corp., Laporte, Colo. [Available at http://eosweb.lard.nasa. gov/PRODOCS/nvap/sci_tech_report_3333.pdf.]

Wang, J., L. Zhang, A. Dai, T. Van Hove, and J. Van Baelon (2007), A near-global, 2-hourly dataset of atmospheric precipitable water from ground-based GPS measurements, *J. Geophys. Res.*, *112*, D11107, doi:10.1029/2006JD007529.

Wentz, F. J., L. Ricciardulli, K. A. Hilburn, and C. A. Mears (2007), How much more rain will global warming bring?, *Science*, *317*, 233–235, doi:10.1126/science.1140746.